Reprinted from September 1985, Vol. 107, Journal of Applied Mechanics

Stability of a Rigid Body With an Oscillating Particle: An Application of MACSYMA

L. A. Month
Department of Mechanical Engineering,
University of California at Berkeley,
Berkeley, Calif. 94720

R. H. Rand
Department of Theoretical
and Applied Mechanics,
Cornell University,
Ithaca, N.Y. 14853
Mem. ASME

This problem is a generalization of the classical problem of the stability of a spinning rigid body. We obtain the stability chart by using: (i) the computer algebra system MACSYMA in conjunction with a perturbation method, and (ii) numerical integration based on Floquet theory. We show that the form of the stability chart is different for each of the three cases in which the spin axis is the minimum, maximum, or middle principal moment of inertia axis. In particular, a rotation with arbitrarily small angular velocity about the maximum moment of inertia axis can be made unstable by appropriately choosing the model parameters. In contrast, a rotation about the minimum moment of inertia axis is always stable for a sufficiently small angular velocity. The MACSYMA program, which we used to obtain the transition curves, is included in the Appendix.

Introduction

This paper concerns the stability of the steady rotation of a rigid body containing a particle that oscillates sinusoidally along a principal axis. In the limiting case where the particle has zero mass, the solution to this problem reduces to the classical result that rotations about the axes of largest and smallest moment of inertia are stable, while a rotation about the middle moment of inertia axis is unstable [3]. The presence of the oscillating particle makes the stability criterion much more complicated.

Mathematically, this problem involves the stability of an equilibrium position in a nonlinear dynamical system that is parametrically driven by a periodic forcing function. Such stability problems may be efficiently investigated by using Floquet theory [9], which yields information about the asymptotic behavior of the system based on the system's performance over one period of the forcing function. Moreover, Floquet theory may be used in the context of perturbation methods to obtain stability criterion in the form of power series expansions in some small parameter.

While such analytical computations are straightforward [9], the grueling algebra involved has limited their use in the past. With the recent advent of computer algebra, however, new possibilities arise. Computer algebra systems such as MACSYMA [8] permit the exact handling of algebraic expressions involving unevaluated variables (represented, as usual, by letters). Differentiation and integration are supported, and, in general, any routine computations that a person can do by hand can now be done with greater speed and accuracy by computer. Moreover, MACSYMA uses exact (rational) arithmetic, so that the roundoff error usually associated with computer solutions is absent.

In this paper we show how such computations can be applied to the problem at hand. We include the listing of a MACSYMA program which computes stability transition curves in the form of power series expansions out to arbitrary order (limited only by the memory size of the computer).

The problem of a rigid body carrying an oscillating particle has been previously investigated by Kane [5]. He derived the governing equations and presented a preliminary stability analysis, obtaining the lowest order approximation for the stability transition curves. He concluded that rotations about the middle moment of inertia axis could be made stable, and that rotations about the largest and smallest moment of inertia axes could be made unstable, by choosing the parameters appropriately.

In this paper we will extend Kane's analysis in two ways. Firstly, we will use computer algebra to develop stability criterion in the form of power series expansions in a small parameter. Secondly, we will use numerical integration in the setting of Floquet theory to obtain results valid over a wider range of parameter values. This work will reveal an entirely unexpected family of regions of stability and instability in the parameter plane. In addition we will show that rotations about the minimum moment of inertia axis have different stability properties than rotations about the maximum moment of inertia axis.

Theory

In this section we set up the problem and derive certain properties of the stability transition curves. We begin by stating the governing equations of motion (from [5]):

Contributed by the Applied Mechanics Division and presented at the 1985 Joint ASME/ASCE Applied Mechanics, Fluids Engineering, and Bioengineering Conference, Albuquerque, N. Mex., June 24-26, 1985 of THE AMERICAN SOCIETY OF MECHANICAL ENGINEERS.

Discussion on this paper should be addressed to the Editorial Department, ASME, United Engineering Center, 345 East 47th Street, New York, N.Y., 10017, and will be accepted until two months after final publication of the paper itself in the JOURNAL OF APPLIED MECHANICS. Manuscript received by ASME Applied Mechanics Division, August, 1984; final revision October, 1984. Paper No. 85-APM-28.

$$(I_2 - I_3)\omega_2\omega_3 - I_1\dot{\omega}_1 = 0$$
$$(I_3 - I_1)\omega_3\omega_1 - I_2\dot{\omega}_2 - s\mu(s(\dot{\omega}_2 - \omega_1\omega_3) + 2\dot{s}\omega_2) = 0$$
$$(I_1 - I_2)\omega_1\omega_2 - I_3\dot{\omega}_3 - s\mu(s(\dot{\omega}_3 + \omega_1\omega_2) + 2\dot{s}\omega_3) = 0 \quad (1)$$

where dots represent differentiation with respect to time t, and where I_i and ω_i are the principal moments of inertia and the corresponding angular velocities, respectively. The particle is assumed to move along the I_1 axis, with $s = s(t)$ as its distance from the center of mass of the rigid body. The parameter $\mu = mM/(m+M)$, where m and M are the masses of the particle and rigid body, respectively.

Throughout this paper we will be interested in the stability of a steady rotation about the axis on which the particle is constrained to move:

$$\omega_1 = \omega = \text{constant}, \quad \omega_2 = 0, \quad \omega_3 = 0. \quad (2)$$

To investigate the stability of this solution, we define the following small deviations from steady state:

$$x_1 = \omega_1 - \omega, \quad x_2 = \omega_2, \quad x_3 = \omega_3. \quad (3)$$

We substitute (3) into (1) and linearize in the x_i to obtain these linear variational equations:

$$d/dt\ x_1 = 0$$
$$d/dt((I_2 + \mu s^2)x_2) + (I_1 - I_3 - \mu s^2)\ \omega x_3 = 0$$
$$d/dt((I_2 + \mu s^2)x_2) + (I_1 - I_3 - \mu s^2)\ \omega x_3 = 0. \quad (4)$$

The solution (2) is said to be stable if all solutions to (4) are bounded, and unstable if an unbounded solution to (4) exists. We may thus ignore the first equation of (4) which cannot produce instability.

We prescribe the motion $s(t)$ of the particle to be sinusoidal,

$$s = s(t) = A \cos \Omega\ t. \quad (5)$$

To nondimensionalize (4), we set

$$J_2 = I_2/I_1, \quad J_3 = I_3/I_1 \quad (6)$$

and define $\tau = \Omega t$, giving

$$(f_2\ x_2)' + g_3 x_3 = 0, \quad (f_3\ x_3)' - g_2\ x_2 = 0 \quad (7)$$

where primes represent differentiation with respect to τ and where, for $i = 2,3$,

$$f_i = J_i + \epsilon \cos^2\tau$$

$$g_i = \sqrt{\frac{K J_2 J_3}{(1-J_2)(1-J_3)}}\,(1 - f_i) \quad (8)$$

in which ϵ and K are dimensionless parameters:

$$\epsilon = \mu\ A^2/I_1 = (mM/(m+M))\ A^2/I_1 \quad (9)$$

$$K = \frac{(1-J_2)(1-J_3)}{J_2 J_3}\,(\omega/\Omega)^2. \quad (10)$$

In the case that $\epsilon = 0$, equations (7) may be written in the form:

$$x_i'' + K x_i = 0, \quad i = 2,3. \quad (11)$$

This limit corresponds to the classical problem in which the particle has no mass or does not move. Equation (11) will have no unbounded solutions only if $K > 0$, i.e., if $(1-J_2)(1-J_3) > 0$, i.e., if the rotation axis has the largest or smallest principal moment of inertia.

Equations (7) thus depend on four dimensionless parameters: ϵ, K, J_2, and J_3. For a particular rigid body, J_2 and J_3 are fixed, while ϵ and K, respectively, reflect the forcing amplitude and the ratio of spin frequency ω to forcing frequency Ω. To reduce the size of the parameter space from 4 to 2, we view J_2 and J_3 as fixed, and are interested in which points in the K-ϵ plane correspond to stable, and which to unstable motions (2). Since $\epsilon > 0$ from (9), we are interested only in the upper half of the K-ϵ plane. Moreover, we note that three distinct cases occur: If $(1-J_2)\ (1-J_3) > 0$ then $K > 0$ and we are interested only in the first quadrant of the K-ϵ plane. We have two cases $J_2 < 1$, $J_3 < 1$ or $J_2 > 1$, $J_3 > 1$. These cases correspond to a rotation about the maximum or minimum moment of inertia axis, respectively. The third case, in which the rotation is about the middle moment of inertia axis, involves $K < 0$ and restricts our attention to the second quadrant of the K-ϵ plane.

In particular we are interested in the transition curves that separate regions of stability from regions of instability in the appropriate quadrant of the K-ϵ plane. On such a curve, it is well known from Floquet theory that there must exist periodic solutions having the period of the forcing function ($= \pi$ from equation (8)), or twice that period. This result follows from the Hamiltonian nature of the problem ([1], p. 203; [9], p. 197): equations (7) may be written in Hamiltonian form,

$$q' = \partial H/\partial p, \quad p' = -\partial H/\partial q \quad (12)$$

where $q = f_3 x_3$, $p = f_2 x_2$, and

$$H = \left(\frac{g_3}{f_3}\,q^2/2 + \frac{g_2}{f_2}\,p^2/2\right).$$

Thus, to find transition curves in the K-ϵ plane, it is sufficient to look for periodic solutions of period π or 2π. We begin by finding those points on the positive K axis from which regions of instability originate. When $\epsilon = 0$, equation (11) shows that equations (7) have period $2\pi/\sqrt{K}$. Hence for a transition point on the positive K axis we require (11) to exhibit solutions with period $2\pi/N$, $N = 0, 1, 2, \ldots$ since all such solutions will have period 2π; (e.g., a solution of period π may also be considered to have period 2π, but not vice versa). $N = 0$ corresponds to a constant solution (which occurs in equations (7) for $K = \epsilon = 0$), which may also be thought of as a periodic function of period 2π. This gives

$$2\pi\sqrt{K} = 2\pi/N \quad \text{or} \quad K = N^2, \ N = 0,1,2, \ldots. \quad (13)$$

For $\epsilon = 0$ and $K < 0$, equation (11) has unbounded solutions, and therefore the entire negative K axis is unstable.

At each of the points $K = N^2$, $\epsilon = 0$, we expect two transition curves to intersect the K axis, the solution on one behaving like $\sin N\tau$, and on the other like $\cos N\tau$ for $\epsilon = 0$. An exception is the $N = 0$ case, where we expect a single transition curve with solution behaving like a constant for $\epsilon = 0$. This situation is so far reminiscent of Mathieu's equation ([2], p. 65),

$$x'' + (\delta + \epsilon \cos 2t)\ x = 0 \quad (14)$$

which is the paradigm for problems in Floquet theory.

We now note a surprising difference between the behavior of equations (7) and the Mathieu equation (14). The $N = 0$ transition curve (which intesects the origin $K = \epsilon = 0$) is the straight line $K = 0$ for equations (7), whereas it is a curved line having a complicated power series expansion in ϵ for Mathieu's equation (see [8]). This may be proved as follows: When $K = 0$, $g_2 = g_3 = 0$ in equation (8), and equations (7) become

$$(f_2\ x_2)' = 0 \quad \text{and} \quad (f_3\ x_3)' = 0. \quad (15)$$

These equations have the general solution

$$x_2 = c_1/f_2 \quad \text{and} \quad x_3 = c_2/f_3 \quad (16)$$

where c_1 and c_2 are arbitrary constants. From equations (8), f_2 and f_3 are periodic with period π, and hence, from Floquet theory, all points on the ϵ axis are transition points.

Note that this implies that for equations (7), stability is not possible for negative K near the origin. This is in contrast to the behavior of Mathieu's equation, in which the transition

curve through $\delta=\epsilon=0$ bends to the left and thus carries a region of stability into the negative K half-plane.

We are interested in using computer algebra to obtain approximate expressions for each of the two transition curves that go through the points $K=N^2$, $\epsilon=0$. Before proceeding with this computation, however, we note a remarkable symmetry property that these transition curves possess.

Theorem: Let

$$K=F(\epsilon;J_2,J_3) \quad \text{and} \quad K=G(\epsilon;J_2,J_3) \tag{17}$$

represent the two transition curves emanating from a single transition point on the K axis. Then the functions F and G interchange when J_2 and J_3 are interchanged:

$$F(\epsilon;J_3,J_2)=G(\epsilon;J_2,J_3) \tag{18}$$

Before proving this theorem, we note that it implies that when $J_2=J_3$, each pair of transition curves emanating from the same point on the K axis coalesce. This means that in the case of a dynamically symmetric rigid body, all the associated regions of instability disappear.

Proof: We begin by writing equations (7) in the form of a single second-order equation. We solve the first of equations (7) for x_3 and substitute into the second, giving:

$$(f_3(f_2\ x_2)'/g_3)'+g_2x_2=0. \tag{19}$$

Alternately, we could have eliminated x_2 giving:

$$(f_2(f_3x_3)'/g_2)'+g_3x_3=0. \tag{20}$$

On a transition curve there exists a solution to equation (19) of period 2π which may be expanded in a Fourier series:

$$x_2(\tau)=\sum_{n=0}^{\infty} a_n\ \cos\ n\tau+b_n\ \sin\ n\tau. \tag{21}$$

We substitute (21) into (19), collect terms, and equate coefficients of $\cos\ n\tau$ and $\sin\ n\tau$ to zero. As in the case of Mathieu's equation (see [9], p. 204), this results in two *uncoupled* sets of homogeneous linear algebraic equations, respectively on the a_n and b_n coefficients. Thus we may obtain an even periodic solution (if all the b_n equal zero) or an odd periodic solution (if all the a_n equal zero), each case giving rise to separate transition curves. If we suppose that on the transition curve $K=F$ in (17), x_2 is an even periodic function, then on $K=G$, x_2 will be odd.

Next we show that whenever $x_2(\tau)$ is even, $x_3(\tau)$ must be odd. We replace τ by $-\tau$ in equation (7) and use $x_2(-\tau)=x_2(\tau)$, giving

$$-(f_2(\tau)\ x_2(\tau))'+g_3(\tau)\ x_3(-\tau)=0,$$
$$-(f_3(\tau)\ x_3(-\tau))'-g_2(\tau)\ x_2(\tau)=0$$

from which it follows that $x_3(-\tau)=-x_3(\tau)$ by comparison with (7).

Finally, we note that when J_2 and J_3 are interchanged, the linear differential operators defined by equations (19) and (20) interchange. Thus

$$x_2(\tau;J_2,J_3)=x_3(\tau;J_3,J_2).$$

This means that the transition curve on which x_2 was even and x_3 was odd interchanges with the one on which x_2 was odd and x_3 was even, i.e., equation (18) holds.

Computer Algebra

We use a well-known perturbation method [9] to obtain approximate expressions for the transition curves that intersect the K axis at $K=N^2$. Our setup and computer algebra implementation will closely follow the treatment of Mathieu's equation ([8], pp. 87–94).

The procedure will be to expand x_2 and K in equation (19) in power series in ϵ. When $\epsilon=0$, equation (19) reduces to equation (11), and has two linearly independent periodic solutions, one even and one odd: $\cos N\tau$ and $\sin N\tau$, where $N=1,2,3,\ldots$ tags the particular transition curves we are approximating. To treat each value of N as similarly as possible, we begin by defining a new independent variable z:

$$z=N\tau. \tag{22}$$

Then when $\epsilon=0$, equation (19) exhibits the solutions $\cos z$ and $\sin z$, independent of N.

Then we expand:

$$K=N^2(1+K_1\ \epsilon+K_2\ \epsilon^2+\ \ldots) \tag{23}$$

$$x_2(z)=x_{20}(z)+x_{21}(z)\ \epsilon+x_{22}(z)\ \epsilon^2+\ \ldots \tag{24}$$

where $x_{20}(z)$ is taken either as $\cos z$ or $\sin z$, each choice giving a distinct transition curve.

The method entails substituting (22)–(24) into (8) and (19), collecting terms, and equating coefficients of powers of ϵ to zero. This yields a sequence of differential equations on the $x_{2i}(z)$. The constants K_i are obtained by requiring the resulting solutions to be bounded (periodic) functions of z. It is sufficient to choose the constants of integration in these equations to be zero, since for a transition curve we are interested in any periodic solution of period π or 2π.

This method involves a great deal of algebra. Even explicitly computing equation (19), which contains 28 terms, would be difficult to do correctly by hand. The substitution of equations (23) and (24), and collection of terms would have been virtually impossible without computer algebra.

The MACSYMA program which we used, and an explanation of how it works, is presented in the Appendix. In the following we present a sample of the program's output, namely an expression for the $N=1$ transition curve corresponding to the choice $x_{20}(z)=\sin z$ expanded out to 0(3). The quantities J_{12} and J_{13} are respectively defined as $1-J_2$ and $1-J_3$:

$$\begin{aligned}
K=1+\ & \frac{(((J_{13}+3J_{12})J_2+J_{12}J_{13})J_3+3J_{12}J_{13}J_2)\epsilon}{4J_{12}J_{13}J_2J_3}\\
&+(((7J_{13}^2+18J_{12}J_{13}+71J_{12}^2)J_2^2\\
&+(-2J_{12}J_{13}^2+18J_{12}^2J_{13})J_2-9J_{12}^2J_{13}^2)J_3^2\\
&+((18J_{12}J_{13}^2+62J_{12}^2J_{13})J_2^2+18J_{12}^2J_{13}^2J_2)J_3\\
&-9J_{12}^2J_{13}^2J_2^2)\epsilon^2/(128J_{12}^2J_{13}^2J_2^2J_3^2)\\
&+(((41J_{13}^3+69J_{12}J_{13}^2+283J_{12}^2J_{13}+1655J_{12}^3)J_2^3\\
&+(-85J_{12}J_{13}^3-102J_{12}^2J_{13}^2+283J_{12}^3J_{13})J_2^2\\
&+(27J_{12}^2J_{13}^2-171J_{12}^3J_{13}^2)J_2+153J_{12}^3J_{13}^3)J_3^3\\
&+((69J_{12}J_{13}^3+166J_{12}^2J_{13}^2+1205J_{12}^3J_{13})J_2^3\\
&+(-102J_{12}^2J_{13}^3+166J_{12}^3J_{13}^2)J_2^2\\
&-171J_{12}^3J_{13}^3J_2)J_3^2+((-117J_{12}^2J_{13}^3\\
&-315J_{12}^3J_{13}^2)J_2^3-117J_{12}^3J_{13}^3J_2^2)J_3\\
&+135J_{12}^3J_{13}^3J_2^3)\epsilon^3/(4096J_{12}^3J_{13}^3J_2^3J_3^3)+\ \ldots.
\end{aligned} \tag{25}$$

As noted previously in property (18), the $N=1$ transition curve corresponding to the choice $x_{20}(z)=\cos z$ is identical to equation (25) with J_2 and J_{12}, respectively, interchanged with J_3 and J_{13}.

Note that in equation (25), J_2 and J_3 are left as algebraic parameters. Inspection of equation (25) and the corresponding expression for the other $N=1$ transition curve suggested property (18) to us, which we were then able to substantiate theoretically.

As another example of the utility of having algebraic expressions like equation (25), we obtained an expression for the width of the region of instability associated with equation (25), and tried to find a condition on J_2 and J_3 (in addition to

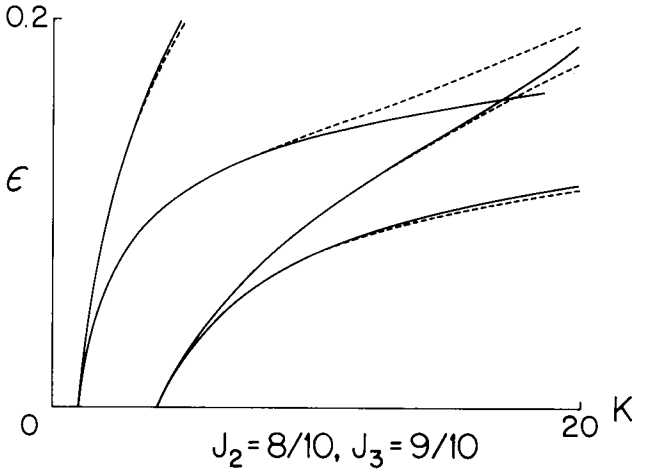

Fig. 1(*a*) $J_2 = 8/10$ and $J_3 = 9/10$. Rotations about maximum axis. The solid lines are analytical expressions for the transition curves. They include terms of 0(8) for $N = 1$ and 0(7) for $N = 2$. The dashed lines represent transition curves calculated numerically.

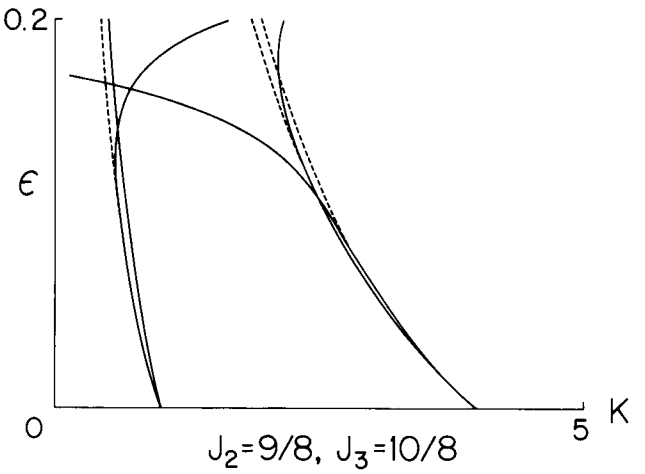

Fig. 1(*b*) $J_2 = 9/8$ and $J_3 = 10/8$. Rotation about minimum axis. The solid lines are analytical expressions for the transition curves. They include terms of 0(8) for $N = 1$ and 0(7) for $N = 2$. The dashed lines represent transition curves calculated numerically.

Fig. 1

the already discussed condition $J_2 = J_3$) which would make this region as small as possible. In the notation of equation (17), we computed $F(\epsilon;J_2,J_3) - G(\epsilon;J_2,J_3)$. We found that while the resulting expression generally had a term or order ϵ, we could eliminate this lowest order term by choosing $J_2 + J_3 = 1$. While this condition does not eliminate the $N = 1$ region entirely (as the $J_2 = J_3$ condition does), it also does not require the body to be dynamically symmetric. In fact, since in physical variables this becomes $I_2 + I_3 = I_1$ (see equation (6)), it can only be applied to situations in which the spin axis is the axis of largest moment of inertia. Incidentally, we note that this condition, $J_2 + J_3 = 1$, does not play any such instability-minimizing role with regard to the $N = 2$ transition region (which generally has a width of order ϵ^2).

This ability of computer algebra programs to leave parameters unevaluated offers a characteristic advantage over traditional computer calculations. However, it takes up a lot of memory. We carried out all these computations on Cornell's DEC 2060 mainframe computer. We found that we could obtain expressions in the form of equation (25) valid to 0(4) before limitations in the computer's memory size stopped us from going further. However, if we assigned J_2 and J_3 numerical values before running the computation, we found we could get results valid to 0(8).

To check our computer algebra computations and to investigate the dynamics of this problem when ϵ is not necessarily small, we used numerical integration.

Numerical Integration

The procedure for using Floquet theory and numerical integration to determine the stability of a first-order system of differential equations (such as equations (7)) is well known [9] and may be outlined as follows:

1. Numerically integrate from 0 to π (= the period of the forcing function) for two sets of initial conditions:
   (*i*) $x_2(0) = 1$, $x_3(0) = 0$, and
   (*ii*) $x_2(0) = 0$, $x_3(0) = 1$.

2. Find the eigenvalues of the resulting fundamental solution matrix M (evaluated at time π). If both eigenvalues have absolute values less than unity, then the motion is stable, and so on.

3. In the case of a Hamiltonian system (cf. equation (12)), the eigencomputation is simplified since the associated matrix M has determinant unity. In this case it is sufficient that the absolute value of the trace of the matrix M be less than 2.

We used a fourth-order Runge-Kutta scheme to implement the preceding algorithm. By choosing various parameter values (we fixed J_2 and J_3, and varied K and ϵ), we were able to approximate the location of transition curves (on which the trace of the matrix M is ± 2).

In what follows, we present some numerical results for a rigid body with principal moments of inertia in the ratio 8:9:10. In the case in which the spin axis is the axis of the largest moment of inertia, this gives $J_2 = 8/10$ and $J_3 = 9/10$. When the spin axis corresponds to the middle moment of inertia, we have $J_2 = 10/9$ and $J_3 = 8/9$. If the spin axis is the axis of the smallest moment of inertia, then $J_2 = 9/8$ and $J_3 = 10/8$.

To begin with, we set $J_2 = 8/10$ and $J_3 = 9/10$ in our MACSYMA program and obtained computer algebra expressions for the first four transition curves ($N = 1$ and 2). As an example, we present the transition curve corresponding to equation (25), but carried out to 0(8):

$$K = 1 + \frac{475\,\epsilon}{48} + \frac{1321375\,\epsilon^2}{18432} + \frac{3429696875\,\epsilon^3}{7077888}$$
$$+ \frac{25933872809375\,\epsilon^4}{8153726976} + \frac{573740794468203125\,\epsilon^5}{28179280429056}$$
$$+ \frac{27429354565142230468 75\,\epsilon^6}{21641687369515008} \qquad (26)$$
$$+ \frac{12676914311735148281640625\,\epsilon^7}{16620815899787526144}$$
$$+ \frac{11832356872679546545169921875\,\epsilon^8}{2692572175765579235328} + \ldots .$$

In addition we obtained analogous expressions for the case $J_2 = 9/8$ and $J_3 = 10/8$. In Figs. 1(*a*) and 1(*b*), we present a plot of the first four computer algebra generated curves (one of which is equation (26)), and we compare them to points obtained by the previously described numerical integration scheme. The agreement is excellent for values of ϵ less than about 0.1.

In Figs. 2–4, we present the results of numerical integration for the cases ($J_2 = 8/10$, $J_3 = 9/10$), ($J_2 = 10/9$, $J_3 = 8/9$), and ($J_2 = 9/8$, $J_3 = 10/8$), respectively. Note the presence of an entire family of transition curves in Fig. 2 that do not intersect the K axis. These curves are not displayed in Fig. 1(*a*) and

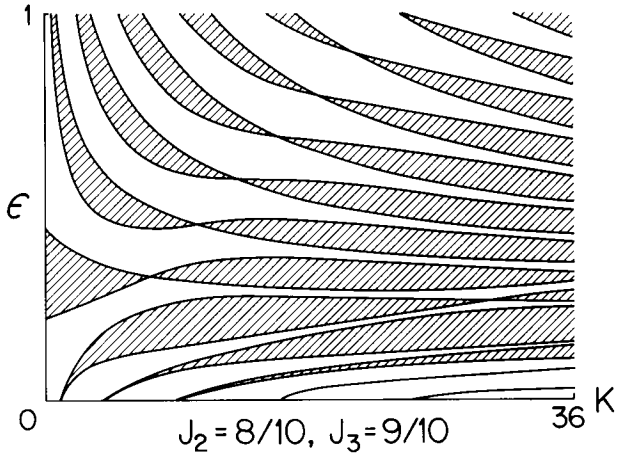

Fig. 2 $J_2 = 8/10$ and $J_3 = 9/10$ stability chart for rotation about maximum principal axis. Here shaded regions are unstable and unshaded regions are stable.

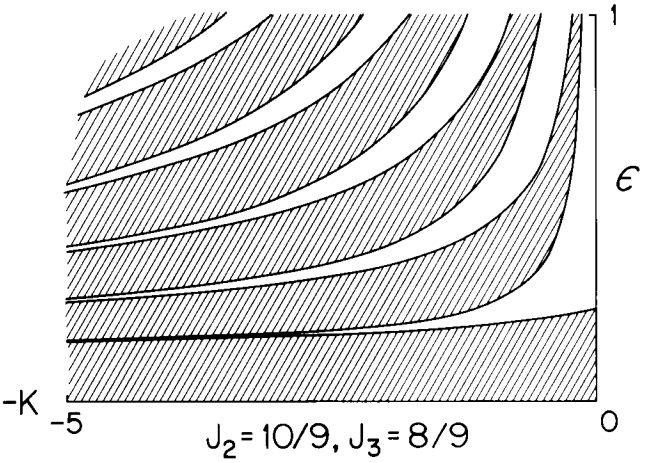

Fig. 3 $J_2 = 10/9$ and $J_3 = 8/9$ stability chart for rotation about middle principal axis. Here shaded regions are unstable and unshaded regions are stable.

cannot be found by a perturbation method, which is based on a small ϵ analysis. Similarly in Fig. 3, there is a family of transition curves, none of which intersect the K axis. (Note that for this case the small ϵ perturbation theory predicts instability for all $K<0$.) In Fig. 4 all the transition curves intersect the K axis.

Note that Fig. 2 predicts that even when the angular velocity ω of the rigid body about its axis of rotation is small (in which case K will be small from equation (10)), instability is possible if the amplitude of the motion of the oscillating particle is appropriately chosen. Similarly in the case of Fig. 3 note that when K is nearly zero the motion can be made stable by choosing the forcing amplitude sufficiently large. In the case of Fig. 4, when K is very small the motion is always stable.

These last considerations are based on the existence of transition curves which intersect the ϵ axis. With the numerical results of Figs. 2-4 as motivation, we look for the points of intersection of these transition curves with the ϵ axis by using a perturbation method.

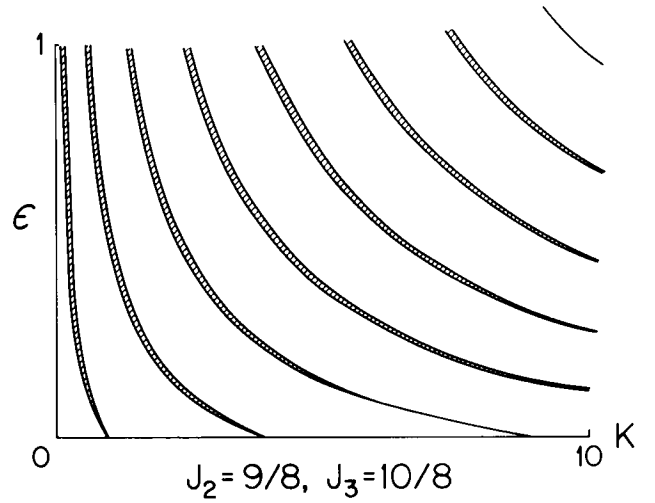

Fig. 4 $J_2 = 9/8$ and $J_3 = 10/8$ stability chart for rotation about minimum principal axis. Here shaded regions are unstable and unshaded regions are stable.

More Perturbations

When K is small, equations (7) simplify because the functions g_i in (8) also become small. For convenience we set, for $i = 2, 3$,

$$g_i = \sqrt{K}\ G_i \tag{27}$$

where $G_i = J^*(1 - f_i)$,

$$J^* = \sqrt{\frac{J_2 J_3}{(1-J_2)(1-J_3)}}.$$

We look for a solution to equations (7) that is valid when K is small by using the two variable expansion method [6]. We replace τ as independent variable by two new variables, ξ and η:

$$\xi = \tau,\ \eta = \sqrt{K}\,\tau. \tag{28}$$

Then

$$\frac{d}{d\tau} = \frac{\partial}{\partial \xi} + \sqrt{K}\ \frac{\partial}{\partial \eta}. \tag{29}$$

We expand $x_2(\xi, \eta)$ and $x_3(\xi, \eta)$ in power series in $\sqrt{K}$:

$$x_i = x_{i0} + \sqrt{K}\, x_{i1} + \ldots \quad i = 2,3. \tag{30}$$

Substituting (29) and (30) into (7) and collecting terms gives:

$$(f_2\, x_{20})_\xi = 0, \quad (f_3\, x_{30})_\xi = 0 \tag{31}$$

$$(f_2\, x_{21})_\xi = -(f_2\, x_{20})_\eta - G_3\, x_{30} \tag{32}$$

$$(f_3\, x_{31})_\xi = -(f_3\, x_{30})_\eta + G_2\, x_{20}. \tag{33}$$

The zeroth-order equations (31) are easily solved:

$$x_{20} = A(\eta)/f_2,\ x_{30} = B(\eta)/f_3. \tag{34}$$

Note that the "constants" of integration (A and B) in equations (34) are functions of the slow time variable η.

Substituting (34) into the first-order equation (32) gives:

$$(f_2\, x_{21})_\xi = -A' - J^*\, B\frac{1-f_3}{f_3} \tag{35}$$

where primes represent differentiation with respect to η.

For equation (35) to have bounded solutions, we require that the right-hand side of (35) have average value zero over one forcing period:

$$-A' - J^* B\left(\frac{1}{\sqrt{(J_3)(J_3+\epsilon)}} - 1\right) = 0 \tag{36}$$

where we have used the fact that

$$\int_0^\pi \frac{1}{f_3}\, d\xi = \int_0^\pi \frac{d\xi}{J_3 + \epsilon \cos^2 \xi} = \frac{\pi}{\sqrt{(J_3)(J_3+\epsilon)}}. \tag{37}$$

A similar treatment of equation (33) gives the condition:

$$-B' + J^* A\left(\frac{1}{\sqrt{(J_2)(J_2+\epsilon)}} - 1\right) = 0. \tag{38}$$

Equations (36) and (38) can be written in the form:

$$A'' + J^{*2}\left(\frac{1}{\sqrt{(J_2)(J_2+\epsilon)}} - 1\right)\left(\frac{1}{\sqrt{(J_3)(J_3+\epsilon)}} - 1\right)A = 0 \quad (39)$$

which will have bounded solutions as long as ϵ does not lie between the critical values:

$$\epsilon = \frac{1-J_2^2}{J_2} \quad \text{and} \quad \epsilon = \frac{1-J_3^2}{J_3}. \quad (40)$$

The preceding analysis was for the case in which J^* was positive, i.e., for rotations about the largest or smallest principal axis. The same analysis can be applied to rotations about the middle principal axis by expanding in a power series in $\sqrt{-K}$, and so on. This results in precisely the same expressions for the critical values (40).

Since ϵ is defined to be positive, the critical values occur only when $1-J_2^2$ or $1-J_3^2 > 0$. Thus we have three cases. If $J_2 < 1$ and $J_3 < 1$ (a rotation about the maximum moment of inertia axis) there are two ϵ intercepts. In fact for $J_2 = 8/10$, $J_3 = 9/10$, equation (40) gives the critical values:

$$\epsilon = 9/20,\ 19/90 \quad (41)$$

in agreement with the numerical results. If $J_2 > 1$ and $J_3 < 1$ (a rotation about the middle moment of inertia axis) there is one transition curve bifurcating from the positive ϵ axis. For $J_2 = 10/9$ and $J_3 = 8/9$, equation (40) gives the values:

$$\epsilon = 17/72,\ -19/90. \quad (42)$$

The positive value is in agreement with the numerical results presented in Fig. 3. If $J_2 > 1$ and $J_3 > 1$ (a rotation about the minimum moment of inertia axis) then there are no ϵ intercepts. The numerical results in Fig. 4 illustrate this case when $J_2 = 9/8$ and $J_3 = 10/8$.

Conclusions

In this investigation of the effects of an oscillating particle on the steady rotation of a rigid body, we have used computer algebra to obtain closed-form analytical approximations for transition curves. These expressions permitted us to draw certain conclusions that would have been hard to ascertain by traditional numerical approaches. For example, we showed that if a dynamically asymmetric rigid body rotates about, and carries an oscillating particle on, its largest principal axis, then the $N=1$ instability region can be made small by choosing the sum of the two smaller principal moments of inertia equal to largest principal moment of inertia, $I_2 + I_3 = I_1$.

Similarly, we used expressions generated by computer algebra to motivate us to show: (*i*) that the symmetric rigid body (for which $I_2 = I_3$) has no regions of instability emanating from points on the K axis, and (*ii*) that the ϵ axis ($K=0$) is an exact transition curve.

We supplemented our computer algebra-perturbation method approach with numerical integration based on Floquet theory. This permitted us to find the structure of the stability chart far from the K axis. Figures 2 and 3 exhibit families of transition curves that are disconnected from those curves that emanate from the K axis. This situation is quite unlike that occurring in Mathieu's equation. Figure 4 does not have transition curves disconnected from the K axis.

In particular we were able to conclude that a rigid body which is slowly rotating about its axis of largest moment of inertia (i.e., one for which K is small), can be made unstable by oscillating a particle along this axis with the appropriate amplitude. Similarly, we found that the normally unstable motion of a rigid body slowly rotating about its axis of middle moment of inertia could be made stable by oscillating a particle along this axis with an amplitude that depended on the system parameters. In contrast the normally stable motion of a rigid body slowly rotating about its axis of minimum moment of inertia remains stable even when a particle oscillating along this axis is added. If K is not small all cases exhibit regions of stability and instability. We also note the surprising result that the presence of the oscillating particle causes the stability properties of a rotation about the minimum moment of inertia axis to be different from that about the maximum moment of inertia axis; cf. Figs. 2 and 4.

Because of the linear nature of the stability analysis, we are not able to predict what the motion will be like once it becomes unstable. Although such questions are certainly of interest in this application, they are not the subject of this paper. These considerations fall under the category of nonlinear parametric excitation, a subject that has just begun to be investigated in much simpler systems [4, 7].

References

1 Arnold, V. I., *Ordinary Differential Equations*, MIT Press, Cambridge, Mass., 1973.

2 Cesari, L., *Asymptotic Behavior and Stability Problems in Ordinary Differential Equations*, 3rd Ed., Springer Verlag, New York, 1971.

3 Goldstein, H., *Classical Mechanics*, Addison Wesley, Reading, Mass., 1980.

4 Holmes, C. A., and Rand, R. H., "Coupled Oscillators as a Model for Nonlinear Parametric Excitation," *Mechanics Research Comm.*, Vol. 8, No. 5, 1981, pp. 263-268.

5 Kane, T. R., "Stability of Steady Rotations of a Rigid Body Carrying an Oscillating Particle," *Proceedings of the 4th U.S. National Congress of Applied Mechanics*, Berkeley, Calif., 1962, pp. 235-238.

6 Kervorkian, J., and Cole, J. D., *Perturbation Methods in Applied Mathematics*, Springer Verlag, New York, 1981.

7 Month, L. A., and Rand, R. H., "Bifurcation of 4:1 Subharmonics in the Nonlinear Mathieu Equation," *Mechanics Research Comm.*, Vol. 9, No. 4, 1982, pp. 233-240.

8 Rand, R. H., *Computer Algebra in Applied Mathematics: An Introduction to MACSYMA*, Pitman, 1984.

9 Stoker, J. J., *Nonlinear Vibrations*, Wiley-Interscience, New York, 1950.

APPENDIX

MACSYMA is a *functional* language, i.e., programs are written in the form of user-defined functions. For an introduction to programming in MACSYMA, see [8]. The program presented in the following consists of a main function, called TC (for Transition Curve) and of eight other functions that are called by TC.

We offer a brief summary of how each of these functions works. TC begins by "killing" Y_0, i.e., by expunging any value that the function $Y_0(z)$ may have had from a previous run. Then some "pattern matching" functions are called to prepare for their use later in the program to solve the perturbation differential equations. Here two rules named C and S are defined, which will provide a particular solution to the nonhomogeneous equation $y'' + y = f(z)$ when $f(z)$ is a sine or cosine. (Although MACSYMA has a differential equation solver called ODE2 as one of its standard functions, it is relatively inefficient time-wise, compared to pattern matching. The authors thank Professor Jim Geer of SUNY Binghamton for suggesting this use of pattern matching.)

Next TC calls INPUT which queues the user to enter the transition curve number and the degree of truncation from the keyboard. The function SETUP1 then performs the expansions (23) and (24) (with a slight change of notation).

TC then calls SETUP2 which contains the expanded differential equation (19). Here MACSYMA was used to derive the listed equation, and then the MACSYMA editor was used to build the rest of the function SETUP2 around the derived equation. This function does the job of substituting the expansions into the differential equation and collecting terms. The perturbation equations are stored in an array called EQ.

Next $Y_0(z)$ is defined as SIN(Z) and a function named FINDTC is called. The latter performs a FOR-DO loop in which the functions STEP1, STEP2, and STEP3 are called. At the Ith stage of the process, STEP1 plugs all the previously

found perturbation results into the Ith perturbation differential equation. The function OUTOFPOIS is used to convert trig expressions like $\cos^2 z$ to the form $(1+\cos 2z)/2$. (We note that OUTOFPOIS, which is part of the MACSYMA Poisson series package, works more efficiently than the function TRIGREDUCE used in [8].)

STEP2 eliminates secular terms and obtains a value for the Ith coefficient in the expansion (23) for K.

STEP3 uses the previously defined pattern matching rules to solve the Ith differential equation.

Finally OUTPUT displays the resulting expression for the transition curve on the video screen.

When the function FINDTC is finished, control is returned to TC, which now defines $Y_0(z)$ to be COS(Z), and FINDTC is once again called.

Here is the program listing (the E-labels that precede the function definitions may be ignored):

(*E4*) TC( ):=(KILL (*Y0*), MATCHDECLARE (NN, TRUE),

DEFRULE $\left(C, \text{COS}\ (NN\,Z), \dfrac{\text{COS}(NN\,Z)}{1-NN\,NN}\right)$,

DEFRULE $\left(S, \text{SIN}\ (\text{NN Z}), \dfrac{\text{SIN}(NN\,Z)}{1-NN\,NN}\right)$, INPUT( ), SETUP1( ),

SETUP2( ), *Y0*(Z):=SIN(Z), FINDTC( ),

Y0(Z):=COS(Z), FINDTC( ),

(*E5*) INPUT( ):=(*N*:

READ ("ENTER TRANSITION CURVE NUMBER *N*"),

M: READ ("ENTER DEGREE OF TRUNCATION"))

(*E6*) FINDTC( ):=(FOR *I* THRU *M*

DO BLOCK (STEP1( ), STEP2( ), PRINT(F_I),

IF $I=M$ THEN GO(END), STEP(3), PRINT(E_I), END),

OUTPUT( ))

(*E7*) SETUP1(1):=(*W*:1, FOR *I* THRU *M* DO *W*: $W+K_IE^I$,

X:*Y0*(Z), FOR *I* THRU *M* DO *X*: $X+Y_I(Z)E^I$)

(*E8*) SETUP2( ):=(TEMP1: EV$\Bigg(-\dfrac{2\,E^3\,X\,\text{COS}^4\left(\frac{Z}{N}\right)\text{SIN}^2\left(\frac{Z}{N}\right)}{J_{13}J_2J_3N^2}$

$+\dfrac{6\,E^2X\,\text{COS}^2\left(\frac{Z}{N}\right)\text{SIN}^2\left(\frac{Z}{N}\right)}{J_2J_3N^2}+\dfrac{2\,E^2\,X\,\text{COS}^2\left(\frac{Z}{N}\right)\text{SIN}^2\left(\frac{Z}{N}\right)}{J_{13}J_2N^2}$

$+\dfrac{2\,E\,X\,\text{SIN}^2\left(\frac{Z}{N}\right)}{J_2N^2}+\dfrac{4\,E^3\,X_Z\,\text{COS}^5\left(\frac{Z}{N}\right)\text{SIN}\left(\frac{Z}{N}\right)}{J_{13}J_2N}$

$-\dfrac{6\,E^2\,X_Z\,\text{COS}^3\left(\frac{Z}{N}\right)\text{SIN}\left(\frac{Z}{N}\right)}{J_2J_3N}+\dfrac{2\,E^2\,X_Z\,\text{COS}^3\left(\frac{Z}{N}\right)\text{SIN}\left(\frac{Z}{N}\right)}{J_{13}J_2N}$

$-\dfrac{2\,E\,X_Z\,\text{COS}\left(\frac{Z}{N}\right)\text{SIN}\left(\frac{Z}{N}\right)}{J_3N}-\dfrac{4\,E\,X_Z\,\text{COS}\left(\frac{Z}{N}\right)\text{SIN}\left(\frac{Z}{N}\right)}{J_2N}$

$-\dfrac{2\,E\,X_Z\,\text{COS}\left(\frac{Z}{N}\right)\text{SIN}\left(\frac{Z}{N}\right)}{J_{13}N}-\dfrac{E^3\,X_{ZZ}\,\text{COS}^6\left(\frac{Z}{N}\right)}{J_{13}J_2J_3}$

$+\dfrac{2\,E^3\,X\,\text{COS}^6\left(\frac{Z}{N}\right)}{J_{13}J_2J_3N^2}-\dfrac{E^3\,W\,X\,\text{COS}^6\left(\frac{Z}{N}\right)}{J_{12}J_{13}^2}+\dfrac{E^2\,X_{ZZ}\,\text{COS}^4\left(\frac{Z}{N}\right)}{J_2J_3}$

$-\dfrac{E^2\,X_{ZZ}\,\text{COS}^4\left(\frac{Z}{N}\right)}{J_{13}J_3}-\dfrac{E^2\,X_{ZZ}\,\text{COS}^4\left(\frac{Z}{N}\right)}{J_{13}J_2}$

$-\dfrac{2\,E^2X\,\text{COS}^4\left(\frac{Z}{N}\right)}{J_2J_3N^2}+\dfrac{2\,E^2\,X\,\text{COS}^4\left(\frac{Z}{N}\right)}{J_{13}J_2N^2}+\dfrac{2\,E^2\,W\,X\,\text{COS}^4\left(\frac{Z}{N}\right)}{J_{12}J_{13}}$

$+\dfrac{E^2\,W\,X\,\text{COS}^4\left(\frac{Z}{N}\right)}{J_{13}^2}+\dfrac{E\,X_{ZZ}\,\text{COS}^2\left(\frac{Z}{N}\right)}{J_3}+\dfrac{E\,X_{ZZ}\,\text{COS}^2\left(\frac{Z}{N}\right)}{J_2}$

$-\dfrac{E\,X_{ZZ}\,\text{COS}^2\left(\frac{Z}{N}\right)}{J_{13}}-\dfrac{2\,E\,X\,\text{COS}^2\left(\frac{Z}{N}\right)}{J_2N^2}$

$-\dfrac{2\,E\,W\,X\,\text{COS}^2\left(\frac{Z}{N}\right)}{J_{13}}-\dfrac{E\,W\,X\,\text{COS}^2\left(\frac{Z}{N}\right)}{J_{12}}$

$+X_{ZZ}+W\,X$, DIFF$\Big)$,

TEMP1 : TAYLOR (TEMP1, E, 0, M),

FOR I THRU M DO EQ_1 : COEFF (TEMP1, E, I))

(*E9*) STEP1(): = (TEMP1 : $EV(EQ_I$,

MAKELIST $\left([E_J, F_J], J, 1, I-1\right)$, DIFF),

TEMP1 : EV(TEMP1, $Z=N\,U$), TEMP1 : OUTOFPOIS (TEMP1),

TEMP1 : $EV\left(\text{TEMP1}, U=\dfrac{Z}{N}\right)\Big)$

(*E10*) STEP2( ) : = (F_1 : SOLVE (COEFF(TEMP1, $Y_0(Z)$), K_I),

TEMP1 : EXPAND (EV(TEMP1, F_I)))

(*E11*) STEP3( ) : = (TEMP1 : $-EV$(TEMP1, $Y_1(Z)=0$),

TEMP1 : APPLYB1 (TEMP1, S), E_1 : $Y_1(Z)$ = APPLYB1 (TEMP1, C))

(*E12*) OUTPUT( ) : = (TEMP1 : N^2

$EV(W$, MAKELIST ($[F_J]$, J, 1, M)),

TEMP1 : TAYLOR (TEMP1, E, 0, M), PRINT ("K=", TEMP1))